Optica Applicata, Vol. XLIII, No. 2, 2013
DOI: 10.5277/oa130209

Near-field multiple optical trapping using high order axially symmetric polarized beams

ZHEHAI ZHOU[1, 2*], QIAOFENG TAN[2], CHANGXI YANG[2], LIANQING ZHU[1]

[1]Beijing Engineering Research Center of Optoelectronic Information and Instruments, Beijing Information Science and Technology University, Beijing 100192, China

[2]State Key Laboratory of Precision Measurement Technology and Instruments, Tsinghua University, Beijing 100084, China

[*]Corresponding author: zhouzhehai@bistu.edu.cn

The near-field multiple optical trapping using high order axially symmetric polarized beams (ASPBs) is studied for the first time. First, a near-field optical trapping scheme is proposed based on the Kretschmann–Raether configuration, and surface plasmon polaritons (SPPs) field distributions excited by incident ASPBs are calculated, which present a multi-focal-spot pattern and the size of spots is much smaller than that of the diffraction limitation. Then, the gradient forces on Rayleigh dielectric particles formed by the multi-focal-spot focused field are computed, which indicates that multiple ultra-small particles with the refractive index higher than that of the ambient medium can be trapped simultaneously on the metal surface. The number and size of trapped particles can be manipulated by flexibly modifying the polarization order of incident beams, which is expected to enhance the capability of traditional optical trapping systems and provide a solution for massively parallel optical trapping of nanometer-sized particles.

Keywords: optical trapping, surface plasmon polaritons, axially symmetric polarized beams.

1. Introduction

In past several years, optical tweezers using cylindrical vector beams (CVBs) have been demonstrated theoretically and experimentally for their better performances than those of traditional optical trapping using scalar beams. QIWEN ZHAN [1, 2] first theoretically studied the optical trapping of dielectric and metallic particles with radially polarized beams. Then some theoretical and experimental results of the optical trapping with CVBs were reported [3–9]. Meanwhile, some special trapping schemes have also been proposed through the manipulation of polarization and phase distributions of incident cylindrical vector beams in order to enhance the trapping performances, such as generation of optical chain [10] and optical cage [11], using double-ring radially polarized beams [12], higher-order radially polarized beams [13] and optical conveyor belts generated by interference of co-propagating and counter-propa-

gating Bessel beams [14, 15]. However, all these single-beam optical tweezers are almost used for individual particle trapping. Also, the very limited field-of-view of high numerical aperture objective lenses commonly employed for optical trapping restricts the number and the size of particles that can be trapped simultaneously. So, a multiple optical trapping using a single vector beam is expected to trap multiple particles at the same time.

On the other hand, some novel vector beams have always been studied, which is expected to lead to some new effects and phenomena that can expand the functionality and enhance the capability of optical systems. One particular example is an axially symmetric polarized beam (ASPB), a kind of space-variant linearly polarized beam with axial symmetry and the symmetry axis is the propagation axis of the light beam [16]. Such beam has a vector-vortex polarization profile and the vector amplitude of the electric field is expressed as

$$\mathbf{E}(r, \phi, z) = E_0(r, z)\left[\cos(P\phi + \phi_0)\mathbf{e}_x + \sin(P\phi + \phi_0)\mathbf{e}_y\right]$$

when traveling in the z axis, where r and ϕ are the cylindrical coordinates, E_0 is the module of the vector amplitude, P is called the polarization order, ϕ_0 is the initial azimuthal angle for $\phi = 0$, and $\mathbf{e}_x$ and $\mathbf{e}_y$ are the unit vectors in the x axis and y axis. Especially, the ASPB with $P = 1$ is so-called cylindrical vector beam which has been greatly studied and applied. Up to date, many methods have also been reported to generate ASPBs, such as using space-variant subwavelength metallic and dielectric gratings [17, 18], liquid-crystal polarization converters [16] and spatial light modulators (SLMs) [19]. And the tightly focusing properties of ASPBs have also been studied theoretically [20–22], and the focused fields for high order ASPBs ($P > 1$) present a multi-focal-spot pattern which is predicted to be useful for multiple optical trapping. But to the best of our knowledge, the detailed theoretical and experimental studies on multiple optical trapping with high order ASPBs have not been presented until now.

In the paper, we propose a novel near-field multiple optical trapping scheme using high order ASPBs. The surface plasmon polariton (SPP) fields excited by incident ASPBs and their corresponding trapping forces on Rayleigh dielectric particles are numerically demonstrated, which shows that multiple nanometer-sized particles can be trapped at the metal surface for their super-resolution multi-focal-spot focusing properties. And the number and size of trapped particles can be manipulated by flexibly modifying the polarization order of incident beams.

2. Trapping scheme and mathematics

Compared to the far-field optical trapping, surface plasmon-based near-field optical trapping have some unprecedented advantages [23], such as enhanced 2D confinement,

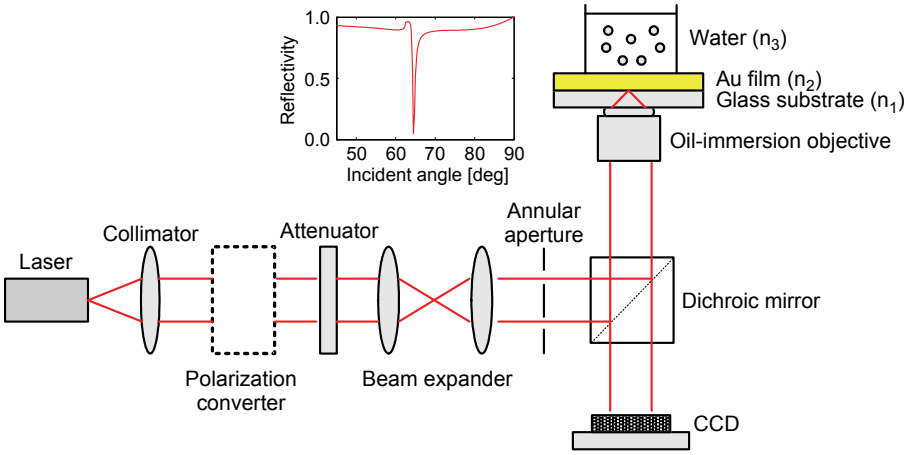

Fig. 1. Schematic diagram of the near-field optical trapping setup.

low energy required for stable trapping and integration with micro-optical devices. Some proposals have been studied theoretically and experimentally [24, 25], such as optical trapping using evanescent fields formed at metal-dielectric interface, sub-wavelength trapping with plasmonic antennas, and self-induced back-action (SIBA) trapping.

In the previous report [26], we briefly studied the SPP excitation by tightly focused high order ASPBs based on the vectorial diffraction theory, which shows that the interfering SPP fields present a multi-focal-spot pattern. Here, we extend the study to near-field multiple optical trapping based on the unique SPP interfering properties, and an optical trapping scheme is proposed based on the Kretschmann–Raether configuration [27] as shown in Fig. 1. In the system, a polarization converter is used to convert the space-invariant linearly polarized beam into a high order ASPB, which is then coupled into an oil-immersion objective lens (such as Olympus, UPLSAPO 100XO, NA = 1.4). The ASPB is focused on the interface between the glass substrate and the Au film, and SPPs can be excited by wavevector-matched *p*-polarized beams at the surface plasmon resonance (SPR) angle θ_{SPR}. The SPP waves propagate radially on the Au film surface and interfere with one another to form a standing wave. An annular aperture placed after the collimated ASPBs provides an annular illumination that blocks the incident angles below the SPR angle.

The reflection and transmission coefficients of the *p* polarization of the above mentioned three-layer system can be expressed as [28],

$$r_p(\theta) = \frac{r_{12}^p(\theta) + r_{23}^p(\theta)\exp\left[i2\sqrt{k_2^2 - k_1^2\sin^2(\theta)}\,d\right]}{1 + r_{12}^p(\theta)r_{23}^p(\theta)\exp\left[i2\sqrt{k_2^2 - k_1^2\sin^2(\theta)}\,d\right]}$$

$$t_p(\theta) = \frac{t_{12}^p(\theta)t_{23}^p(\theta)\exp\left[i\sqrt{k_2^2 - k_1^2\sin^2(\theta)}\ d\right]}{1 + r_{12}^p(\theta)r_{23}^p(\theta)\exp\left[i2\sqrt{k_2^2 - k_1^2\sin^2(\theta)}\ d\right]}$$

where k_1, k_2 and k_3 are the wave numbers in the glass, Au film and water, respectively, d is the thickness of the Au thin film, r_{ij}^p and t_{ij}^p are the reflection and transmission Fresnel coefficients of the p polarization of each of the two respective layer interfaces. Then, the transmitted field on the film surface can be expressed as [26],

$$\mathbf{E}_{\mathrm{SPP}}(r_S, \phi_S, z_S) = \begin{bmatrix} E_r^S(r_S, \phi_S, z_S) \\ E_z^S(r_S, \phi_S, z_S) \end{bmatrix} = A\int_{\theta_{\min}}^{\theta_{\max}} BC\,\mathrm{d}\theta$$

where

$$A = -i^{(3P+1)}\frac{f\pi E_0}{\lambda}$$

$$B = l_0(\theta)\sqrt{\cos(\theta)}\ \sin(\theta)\exp\left[iz_s\sqrt{k_3^2 - k_1^2\sin^2(\theta)}\right]t_p(\theta)\cos\left[(P-1)\phi_S + \phi_0\right]$$

$$C = \begin{bmatrix} \cos(\theta)\left[J_P\left(k_1 r_S\sin(\theta)\right) - J_{P-2}\left(k_1 r_S\sin(\theta)\right)\right] + J_P\left(k_1 r_S\sin(\theta)\right) - J_{P-2}\left(k_1 r_S\sin(\theta)\right) \\ 2i\sin(\theta)J_{P-1}\left(k_1 r_S\sin(\theta)\right) \end{bmatrix}$$

where $S(r_S, \phi_S, z_S)$ is an observation point near the Au film surface, E_r^S and E_z^S are the amplitudes of the radial component and the longitudinal component at point S. $A = f\pi E_0/\lambda$ is a constant, f is the focal length of the objective lens, E_0 is the amplitude of the incident field, and λ is the wavelength in vacuum; $k = 2n\pi/\lambda$ is the wave number, and n is the refractive index of the surrounding medium; θ denotes the focusing angle (the angle between the optical axis and the propagation vector), so $\theta_{\min}$ and $\theta_{\max}$ are the minimum and maximum focusing angle of the focused beam corresponding to annular illumination; P is the polarization order of the incident ASPB, and J_P is the Bessel function of the first kind of the order P, and $l_0(\theta)$ is the pupil apodization function which denotes the relative amplitude and phase of the incident beam.

The SPP interfering fields can exert radiation pressure on particles inside. Especially, in the Rayleigh regime when the radius of the trapped particle is much smaller than the wavelength of the laser, the radiation force can be calculated according to the Rayleigh scattering theory. Here, we assume spherical dielectric

particles with the radius of a ($a \ll \lambda$) to be trapped, then the gradient force $\mathbf{F}_{\text{grad}}$ and the scattering force $\mathbf{F}_{\text{scat}}$ can be expressed as [29],

$$\mathbf{F}_{\text{grad}}(r) = \text{Re}(\gamma)\varepsilon_0 \nabla \mathbf{I}(\mathbf{r})$$

$$\mathbf{F}_{\text{scat}}(\mathbf{r}) = \frac{n_m \langle \mathbf{S} \rangle C_{\text{scat}}}{c}$$

and

$$\gamma = \frac{4\pi a^3 \varepsilon_m (\varepsilon_m - \varepsilon_p)}{\varepsilon_p + 2\varepsilon_m}$$

$$C_{\text{scat}} = \frac{k^4 |\gamma|^2}{6\pi}$$

where γ is the polarizability of the particle, ε_p and ε_m are the relative permittivities of the particle and the surrounding media, respectively; C_{scat} is the scattering cross-section; I is the field intensity, $\langle \mathbf{S} \rangle$ is the time-averaged Poynting vector of the focused beam, and ε_0 and c are the permittivity and light speed in the vacuum, respectively; Re(γ) represents the real part of a complex number. With the above equations, the radiation forces on a Rayleigh dielectric microsphere produced by SPP interfering fields excited by tightly focused ASPBs can be calculated numerically.

3. Numerical results

First, in the trapping system, a 45 nm gold (Au) thin film with a complex permittivity of approximately $-52.02 + 3.87i$ at the wavelength of 1064 nm is considered for deposition on a glass substrate, and the trapped particles are immersed in the water solution. Then the theoretical reflection curve is calculated as shown in inset of Fig. 1, and the SPR angle θ_{SPR} is approximately 64.5° seen from the results.

Further, we choose the wavelength $\lambda = 1064$ nm, $n_3 = n_m = 1.33$, $a = 50$ nm, the numerical aperture (NA) of the oil-immersion lens 1.40, and the total incident power 1 W ($A \approx 10^{11}$ V/m^2) at the pupil. Figures 2**a** and 2**b** demonstrate numerically the SPP field intensity distributions ($I = |E|^2$) at the film surface when the polarization order of incident ASPB is 10 and the pupil apodization function is chosen as

$$l_0(\theta) = \exp\left(\frac{-\sin^2(\theta)}{\sin^2(\alpha)}\right) J_P\left(\frac{\sin(\theta)}{\sin(\alpha)}\right)$$

where $\alpha = \text{asin}(\text{NA}/n)$ is the maximal focusing angle of the focusing beam and $\alpha = 72°$ is chosen in the simulations. Obviously, the SPP fields formed by tightly focused high

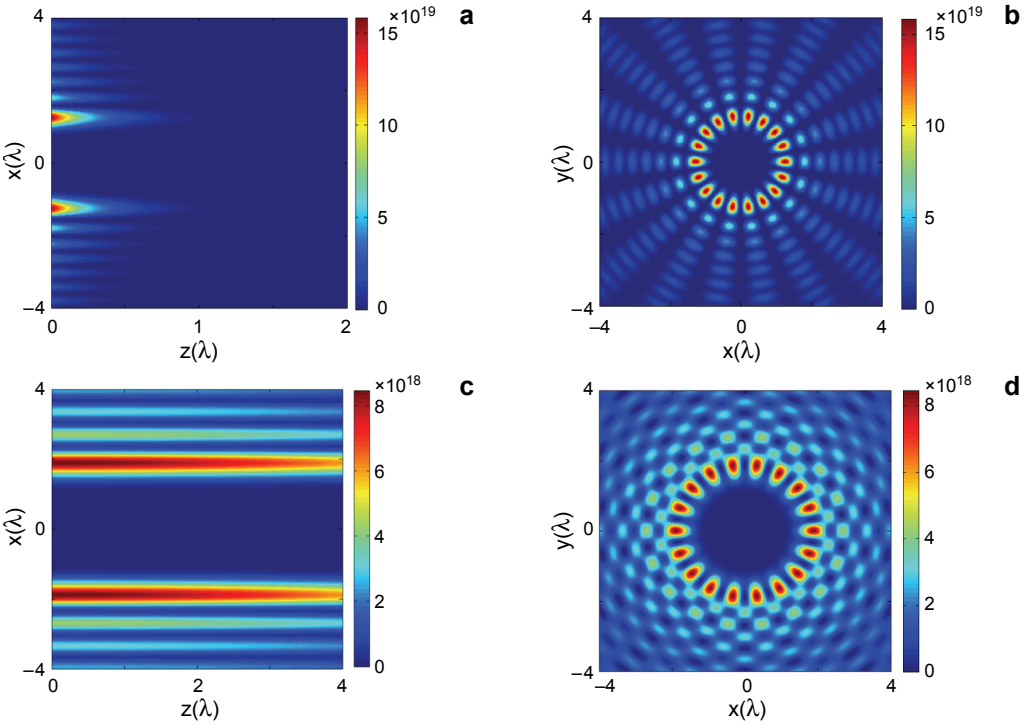

Fig. 2. SPP field distributions on the film surface (**a**) and along the z axis (**b**), and the focused field intensity distributions on the glass surface (**c**) and along the z axis (**d**) without the metal film, where $\theta_{\min} = 62°$, $\theta_{\max} = 67°$, NA = 1.40, $P = 10$, $\phi_0 = 0$.

order ASPBs present a multi-focal-spot pattern, and the number of spots is also related with the polarization order P as $2\times(P-1)$, and the SPP field is confined near the film surface. More interestingly, the size of focused spots is much smaller than that of focused spots formed in the far-field. The FWHM (full width at half maximum) of spots is nearly 0.24λ in the radial direction and 0.12λ in the longitudinal direction, which are both far beyond the Rayleigh diffraction limit. It is worth noticing that there are many side-lobes beside each main lobe, which may be used to trap much more particles under suitable conditions. The super-resolution multi-focal-spot interfering fields are preferred to trap multiple nanometer-sized particles simultaneously. Meanwhile, compared to the focusing without the metal film (called far-field focusing here) as shown in Figs. 2**c** and 2**d**, the field enhancement by about two orders of magnitude is also achieved because of the SPR, which also results in more stable trapping. And higher field enhancement can be obtained by choosing more proper excitation conditions, such as a right type of metal and its thickness.

The radiation force can be calculated according to the Rayleigh scattering theory when spherical Rayleigh dielectric particles ($a \ll \lambda$) are placed in the SPP field. Figure 3 shows the calculated gradient forces produced by SPP fields on two different

types of particles, with a high refractive index 1.60 and a low refractive index 1.10, respectively. For particles with a refractive index higher than that of the ambient medium, there exist multiple equilibrium points at main-lobes and side-lobes where the particles can be trapped. However, for particles with a refractive index lower than the ambient, they cannot be trapped at these spots because of non-equilibrium, but may be trapped at the center and move freely along the longitudinal direction.

In addition, compared with the results without the metal film (called the far-field trapping here) as shown in Fig. 4, there are more equilibrium points at main-lobes and

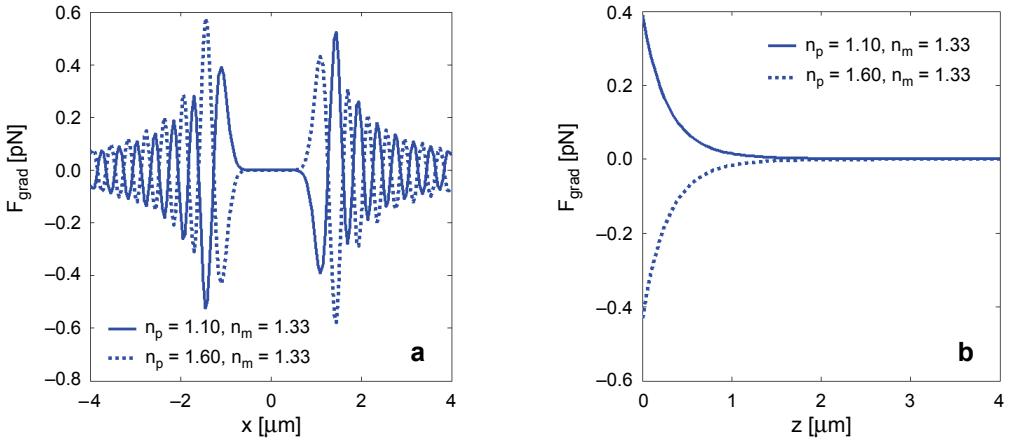

Fig. 3. Gradient forces produced by SPP fields on two different types of particles, where the refractive indices of particles are 1.10 and 1.60, respectively, gradient force along the *x* axis at focus (**a**) and along the *z* axis through focus (**b**).

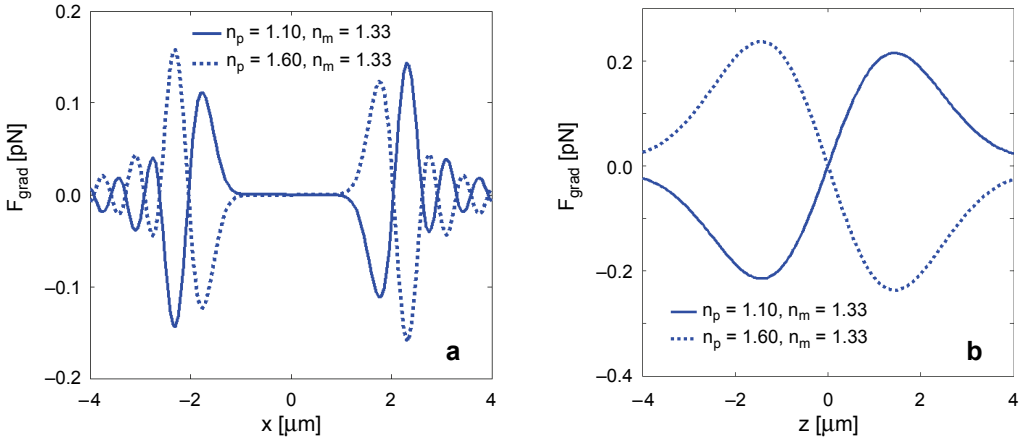

Fig. 4. The gradient forces along the *x* axis at focus (**a**) and along the *z* axis through focus (**b**) produced by the focused fields on two different types of particles without the metal film. The calculated parameters are the same as those in Fig. 3.

side-lobes where the particles can be trapped for particles with refractive index higher than that of the ambient, which means much more particles can be trapped than far-field optical trapping. And the gradient force is also bigger because of the field enhancement.

To achieve a stable trap, some conditions should be satisfied [30]. First, the gradient force F_{grad} should be larger than the scattering force F_{scat}. Generally, the ratio $R_{\text{force}} = = (F_{\text{grad}})_{\max}/(F_{\text{scat}})_{\max}$ is used to estimate the stability for a more conservative estimation, where R_{force} is called the stability criterion. Another condition is that the potential well generated by the gradient forces must be deep enough to overcome the kinetic energy of the trapping particle in Brownian motion, which generally requires $R_{\text{thermal}} = = \exp(-U_m/k_BT) \approx 1$, where k_B is Boltzmann constant and the maximum depth of the potential well U_m can be calculated as $|\text{Re}(\gamma)\varepsilon_0 I_{\max}/2|$. When the particle size is small, the stability criterion can easily be satisfied for trapping of particles with high refractive index as discussed in Ref. [1], so only gradient force should be considered in our simulation. We calculate the R_{force} and R_{thermal} for dielectric particles along the x axis and z axis when the radius is 50 nm and n_p is 1.60. R_{force} along the x axis and z axis are 6.60×10^{51} and 1.38×10^{41}, and R_{thermal} is 1.55×10^{-91}, which obviously demonstrates the stable trap in the situation.

In addition, heating effect owing to high optical intensity should be considered in some cases [31, 32], and a local temperature increase above the boiling point of water could lead to bubble formation and very strong hydrodynamic effects disrupting the trapped particle. The incident optical intensity has to be decreased in order to achieve a small temperature change, but making the trap unstable at the same time. Therefore, the interplay between optical forces and heating for trapped particles should be further explored in future work.

4. Conclusions

In summary, the near-field multiple optical trapping using high order ASPBs has been proposed and demonstrated numerically, which shows that multiple nanometer-sized particles with the refractive index higher than that of the ambient medium can be trapped simultaneously on the metal surface. And compared with the far-field optical trapping, the near-field optical trapping system can trap much smaller and much more particles. Especially, the number of trapped particles can be flexibly manipulated by changing the polarization order of ASPBs, which can be implemented using some devices such as SLMs. The multiple optical trapping with high order ASPBs is expected to enhance the capability of traditional optical trapping systems.

Acknowledgement – The work was supported by the National Natural Science Foundation of China (Nos. 61108047 and 60908015), Beijing Excellent Talent Training Project (No. 2011D005007000008), General Program of Beijing Municipal Commission of Education (No. KM201110772005) and the National Basic Research Program of China (No. 2007CB935303).

References

[1] QIWEN ZHAN, *Radiation forces on a dielectric sphere produced by highly focused cylindrical vector beams*, Journal of Optics A: Pure and Applied Optics **5**(3), 2003, pp. 229–232.

[2] QIWEN ZHAN, *Trapping metallic Rayleigh particles with radial polarization*, Optics Express **12**(15), 2004, pp. 3377–3382.

[3] VOLPE G., SINGH G.P., PETROV D., *Optical tweezers with cylindrical vector beams produced by optical fibers*, Proceedings of SPIE **5514**, 2004, pp. 283–292.

[4] KAWAUCHI H., YONEZAWA K., KOZAWA Y., SATO S., *Calculation of optical trapping forces on a dielectric sphere in the ray optics regime produced by a radially polarized laser beam*, Optics Letters **32**(13), 2007, pp. 1839–1841.

[5] YSHAOHUI YAN, BAOLI YAO, *Radiation forces of a highly focused radially polarized beam on spherical particles*, Physical Review A **76**(5), 2007, article 053836.

[6] NIEMINEN T., HECKENBERG N., RUBINSZTEIN-DUNLOP H., *Forces in optical tweezers with radially and azimuthally polarized trapping beams*, Optics Letters **33**(2), 2008, pp. 122–124.

[7] MICHIHATA M., HAYASHI T., TAKAYA Y., *Measurement of axial and transverse trapping stiffness of optical tweezers in air using a radially polarized beam*, Applied Optics **48**(32), 2009, pp. 6143–6151.

[8] KOZAWA Y., SATO S., *Optical trapping of micrometer-sized dielectric particles by cylindrical vector beams*, Optics Express **18**(10), 2010, pp. 10828–10833.

[9] ROXWORTHY B.J., TOUSSAINT K.C. JR, *Optical trapping with π-phase cylindrical vector beams*, New Journal of Physics **12**(7), 2010, article 073012.

[10] YIQIONG ZHAO, QIWEN ZHAN, YANLI ZHANG, YONG-PING LI, *Creation of a three-dimensional optical chain for controllable particle delivery*, Optics Letters **30**(8), 2005, pp. 848–850.

[11] XI-LIN WANG, JIANPING DING, JIAN-QI QIN, JING CHEN, YA-XIAN FAN, HUI-TIAN WANG, *Configurable three-dimensional cage generated from cylindrical vector beams*, Optics Communications **282**(17), 2009, pp. 3421–3425.

[12] YAOJU ZHANG, BIAOFENG DING, SUYAMA T., *Trapping two types of particles using double-ring-shaped radially polarized beam*, Physical Review A **81**(2), 2010, article 023831.

[13] YOUYI ZHUANG, YAOJU ZHANG, BIAOFENG DING, SUYAMA T., *Trapping Rayleigh particles using highly focused high-order radially polarized beams*, Optics Communications **284**(7), 2011, pp. 1734–1739.

[14] ČIŽMÁR T., GARCÉS-CHÁVEZ V., DHOLAKIA K., ZEMÁNEK P., *Optical conveyor belt for delivery of submicron objects*, Applied Physics Letters **86**(17), 2005, article 174101.

[15] ČIŽMÁR T., KOLLÁROVÁ V., BOUCHAL Z., ZEMÁNEK P., *Sub-micron particle organization of self-imaging of non-diffracting beams*, New Journal of Physics **8**(3), 2006, article 43.

[16] STALDER M., SCHADT M., *Linearly polarized light with axial symmetry generated by liquid-crystal polarization converters*, Optics Letters **21**(23), 1996, pp. 1948–1950.

[17] BOMZON Z., KLEINER V., HASMAN E., *Formation of radially and azimuthally polarized light using space-variant subwavelength metal stripe gratings*, Applied Physics Letters **79**(11), 2001, pp. 1587–1589.

[18] BOMZON Z., BIENER G., KLEINER V., HASMAN E., *Radially and azimuthally polarized beams generated by space-variant dielectric subwavelength gratings*, Optics Letters **27**(5), 2002, pp. 285–287.

[19] XI-LIN WANG, JIANPING DING, WEI-JIANG NI, CHENG-SHAN GUO, HUI-TIAN WANG, *Generation of arbitrary vector beams with a spatial light modulator and a common path interferometric arrangement*, Optics Letters **32**(24), 2007, pp. 3549–3551.

[20] ZHEHAI ZHOU, QIAOFENG TAN, GUOFAN JIN, *Focusing of high polarization order axially-symmetric polarized beams*, Chinese Optics Letters **7**(10), 2009, pp. 938–940.

[21] RASHID M., MARAGO O.M., JONES P.H., *Focusing of high order cylindrical vector beams*, Journal of Optics A: Pure and Applied Optics **11**(6), 2009, article 065204.

[22] KUN HUANG, PENG SHI, CAO G.W., KE LI, ZHANG X.B., LI Y.P., *Vector-vortex Bessel–Gauss beams and their tightly focusing properties*, Optics Letters **36**(6), 2011, pp. 888–890.
[23] RIGHINI M., GIRARD C., QUIDANT R., *Light-induced manipulation with surface plasmons*, Journal of Optics A: Pure and Applied Optics **10**(9), 2008, article 093001.
[24] JUAN M.L., RIGHINI M., QUIDANT R., *Plasmon nano-optical tweezers*, Nature Photonics **5**(6), 2011, pp. 349–356.
[25] MIN GU, HAUMONTE J. B., MICHEAU Y., CHON J.W.M., XIAOSONG GAN, *Laser trapping and manipulation under focused evanescent wave illumination*, Applied Physics Letters **84**(21), 2004, pp. 4236–4238.
[26] ZHEHAI ZHOU, QIAOFENG TAN, GUOFAN JIN, *Surface plasmon interference formed by tightly focused higher polarization order axially symmetric polarized beams*, Chinese Optics Letters **8**(12), 2010, pp. 1178–1181.
[27] RAETHER H., *Surface Plasmons on Smooth and Rough Surfaces and Gratings*, Springer-Verlag, Berlin, 1988, pp. 63–70.
[28] Born M., Wolf E., *Principles of Optics*, 6th Edition, Pergamon Press, Oxford, 1980, pp. 80–110.
[29] HARADA Y., ASAKURA T., *Radiation force on a dielectric sphere in the Rayleigh scattering regime*, Optics Communications **124**(5–6), 1996, pp. 529–541.
[30] ASHKIN A., DZIEDZIC J. M., BJORKHOLM J. E., CHU S., *Observation of a single-beam gradient force optical trap for dielectric particles*, Optics Letters **11**(5), 1986, pp. 288–290.
[31] PLOSCHNER M., MAZILU M., KRAUSS T. F., DHOLAKIA K., *Optical forces near a nanoantenna*, Journal of Nanophotonics **4**(1), 2010, article 041570.
[32] RIGHINI M., GHENUCHE P., CHERUKULAPPURATH S., MYROSHNYCHENKO V., GARCÍA DE ABAJO F.J., QUIDANT R., *Nano-optical trapping of Rayleigh particles and* Escherichia coli *bacteria with resonant optical antennas*, Nano Letters **9**(10), 2009, pp. 3387–3391.

Received March 20, 2012
in revised form July 29, 2012